International Journal of Pharmaceutics 423 (2012) 213–225

Contents lists available at SciVerse ScienceDirect

International Journal of Pharmaceutics

journal homepage: www.elsevier.com/locate/ijpharm

Improvement of flow and bulk density of pharmaceutical powders using surface modification

Laila J. Jallo, Chinmay Ghoroi, Lakxmi Gurumurthy, Utsav Patel, Rajesh N. Davé*

New Jersey Center for Engineered Particulates, New Jersey Institute of Technology, 138 Warren Street, Newark, NJ 07102-1982, USA

ARTICLE INFO

Article history:
Received 28 July 2011
Received in revised form 1 December 2011
Accepted 2 December 2011
Available online 17 December 2011

Keywords:
Dry coating
Design of experiment
Flow properties
Pharmaceutical powders
Cohesion

ABSTRACT

Improvement in flow and bulk density, the two most important properties that determine the ease with which pharmaceutical powders can be handled, stored and processed, is done through surface modification. A limited design of experiment was conducted to establish a standardized dry coating procedure that limits the extent of powder attrition, while providing the most consistent improvement in angle of repose (AOR). The magnetically assisted impaction coating (MAIC) was considered as a model dry-coater for pharmaceutical powders; ibuprofen, acetaminophen, and ascorbic acid. Dry coated drug powders were characterized by AOR, particle size as a function of dispersion pressure, particle size distribution, conditioned bulk density (CBD), Carr index (CI), flow function coefficient (FFC), cohesion coefficient using different instruments, including a shear cell in the Freeman FT4 powder rheometer, and Hansen flowability index. Substantial improvement was observed in all the measured properties after dry coating relative to the uncoated powders, such that each powder moved from a poorer to a better flow classification and showed improved dispersion. The material intrinsic property such as cohesion, plotted as a function of particle size, gave a trend similar to those of bulk flow properties, AOR and CI. Property improvement is also illustrated in a phase map of inverse cohesion (or FFC) as a function of bulk density, which also indicated a significant positive shift due to dry coating. It is hoped that such phase maps are useful in manufacturing decisions regarding the need for dry coating, which will allow moving from wet granulation to roller compaction or to direct compression based formulations.

1. Introduction

Manufacturing of pharmaceutical solid dosage forms involves several processes including flow through hoppers, sieving, pouring, blending, die-filling, and compaction (Guerin et al., 1999). These processes are highly sensitive to powder properties like flowability and bulk density, which are to some extent inter-related, and thus affect the quality of the final product. For example, the die-filling process is affected by the cohesiveness of the powder, which determines the ease with which the powder can be fed into the die (Guerin et al., 1999). Cohesiveness also causes the non-uniformity of the API mass in the tablets (Lindberg et al., 2004). Powder bulk properties and its compressibility also impact the pre-compaction and compaction processes. Thus, flow properties of pharmaceutical powders are critical to manufacturing. Poor flow often causes undesirable process breakdown thereby directly impacting the product uniformity.

Most active pharmaceutical ingredients (APIs) used these days are fine powders 100 μm or less which typically have a wide size distribution. Further, particles smaller than 30 μm are extremely difficult to handle and are a generic problem for the industry (Yang et al., 2005). This is due mostly to the presence of strong inter-particle interactions like van der Waals, capillary and electrostatic forces. For fine dry particles, the van der Waals interaction is the most significant force responsible for cohesiveness of powder (Jallo et al., 2011). To ease the handling of these fine powders, methods like aeration and vibration are used along with the addition of small amounts of flow additives or glidants (Molerus, 1978; Kono et al., 1990; Kaya et al., 1983; Elbicki and Tardos, 1998; Wassgren et al., 2002; Fraige et al., 2008; Pingali et al., 2011). However, these methods could also result in segregation, or non-uniform distribution of the flow additives in the bulk. The use of flow additives may also lead to other disadvantages such as inconsistency in performance and difficulty in predicting the flow behavior a priori. In order to alleviate such disadvantages, dry coating via surface modification has been proposed as an alternate approach where nano-particles are uniformly coated on the surface of the carrier particles (Beach et al., 2010; Yang et al., 2005; Pfeffer et al., 2001).

Surface modification is a technique that reduces the cohesiveness of fine particles substantially by forming a film or thin coating of nano particles on the surface of the particles (Chen et al., 2008, 2009). Surface modification can be achieved through wet or dry

* Corresponding author. Tel.: +1 973 596 5870; fax: +1 973 642 7088.
E-mail address: dave@adm.njit.edu (R.N. Davé).

0378-5173/$ – see front matter © 2011 Elsevier B.V. All rights reserved.
doi:10.1016/j.ijpharm.2011.12.012

methods (Jallo et al., 2010; Pfeffer et al., 2001). The wet processes however, are not environmentally friendly as compared to the dry ones, which are environmentally benign (Lecoq et al., 2011; Pfeffer et al., 2001). Further, for the purpose of flow improvement, dry processes may be more favorable as shown through previously proposed contact models (Chen et al., 2010; Jallo et al., 2011). The dry method has been successfully used to coat different types of cohesive powders and improve their flow (Ramlakhan et al., 2000; Yang et al., 2005; Jallo et al., 2010; Han et al., 2011; Zhou et al., 2011; Lecoq et al., 2011; Mullarney et al., 2011). In the dry coating technique, nano-size (guest) particles are successfully attached to the surface of the cohesive (host) particles to reduce the inter-particle forces without using any solvent, binder or involvement of water (Ramlakhan et al., 2000). The force of attraction between the host and guest particles, which keeps them in contact, is the van der Waals force. The guest particles stay on the surface of the host particle because the force of attraction between the two is greater than the weight of the guest particle (Yu et al., 2003). In addition to inter-particle force reduction, the dry coating technique also results in the improvement of bulk properties such as flowability, bulk density, compressibility. Pharmaceutical powders having these tailor-made properties are most desirable for successful process and product design (Thalberg et al., 2004).

Dry coating generally involves high impaction mechanical force (Pfeffer et al., 2001; Lecoq et al., 2011), which attaches nano-size guest particles to the surface of the host particle. However, since pharmaceutical powders are organic, they are relatively soft or brittle in nature and also sensitive to the heat generated during the high impaction by the coating process (Ramlakhan et al., 2000). Severe processing conditions can lead to reduction in size of the API particles, which is counter-productive to the goal of improving the flow properties. Thus, it is desirable to investigate and employ the standardized use of a dry coating method which can attach the nano-size guest particles onto the host API particles with minimum degradation of particle size, shape and composition for pharmaceutical applications (Ramlakhan et al., 2000). Yang et al. (2005) studied several dry coating devices like the hybridizer, V-blender, and magnetically assisted impaction coating (MAIC) and even dry coating by hand mixing. They found that the MAIC device is the most effective dry coater among the above-mentioned devices, and may cause the least attrition while providing very good property improvement. Previously, under certain processing conditions, MAIC has been utilized to coat some organic host particles (mostly spherical in shape with a narrow size distribution) without causing major changes in the material shape and size (Ramlakhan et al., 1998). However, those powders, such as cornstarch were found to be naturally resistant to attrition due to their elastic properties. The earlier studies also established that to reduce the cohesive force among fine host particles, a discrete coating of nano-size guest particles is sufficient, with surface area coverage (SAC) of as little as 10–20% (Yang et al., 2005). However, those reports did not examine the use of MAIC and other devices for coating active pharmaceutical ingredient (API) powders. Recently, Beach et al. (2010), dry coated acetaminophen as a model API powder in the MAIC and examined the flow properties of different blends of lactose and the surface modified API powders. Most importantly, Beach et al. (2010), demonstrated successful use of Near-IR in-line imaging to examine flow and flow uniformity for regular and dry coated API blends. It was shown that examination of the flow intensity from NIR spectra (inverse signal to noise ratio of spectra) and its standard deviation revealed that dry particle coated blends showed better uniformity of flow as compared to the other methods. Thus they showed that Near-IR may be used as a Process Analytical Technology tool helping promote quality by design. In addition, flow rates of 100% APIs and their blends were also measured and reported, indicating that dry coated powders exhibited enhanced flow rates. In terms of other flow indices, they only utilized the angle of repose measurements, which corroborated Near-IR results, showing that the majority of the blends prepared from coated APIs stayed in either passable or fair category. However, in that study, the MAIC operating condition was not optimized for API coating and particle sizes were not examined to investigate the extent of attrition. Nonetheless, all these studies showed that there are several critical operating parameters affecting the coating performance of the MAIC device (Ramlakhan et al., 2000; Beach et al., 2010). According to those studies, once the host and guest particles are specified, the key parameters that control the operation and performance of the MAIC are mass ratio of host and guest particles, magnet to powder mass ratio, operating voltage, and processing time.

The main objective of this paper is to carry out a comprehensive investigation of the dry coating approach to improve flow and several other related properties of API powders, while limiting the extent of attrition that is expected from such dry coating devices. MAIC is selected as the model dry coating device, which is also considered to be a material-sparing dry coating device based on our recent work (Ghoroi et al., 2010a, 2010b). These studies along with previous reports indicated that the MAIC, when used in conjunction with selected powder flow testers, works as a screening device to determine the feasibility of certain host–guest combinations for achieving the desired improvement of flow properties. Improvement of flow properties of both uncoated (original; as received) and surface modified APIs were quantified via bulk properties using different powder flow testers. Since one of the objectives is to limit attrition, we also evaluated particle size and size distribution before and after coating. This was done using a venturi-tube type device, namely, the Rodos system coupled with laser diffraction measurements where the powder sample was subjected to varying dispersion pressures. This allows for examination of attrition as well as the extent of powder dispersion, when d_{50} and d_{90} particles sizes are plotted as a function of dispersion pressure.

The presentation in this paper is divided into two parts. The first part of the paper is devoted to the optimization of the operating parameters of the MAIC for dry coating of model cohesive APIs using a limited design of experiments (DOE). The model drugs used for the optimization study were Ibuprofen 110, and Acetaminophen (both micronized and coarse grade) which covers particle sizes from 10 to 120 μm. The major contribution of the paper is in the second part, where several API powders like Ibuprofen 110, Ibuprofen 90, Ibuprofen 50, Coarse Acetaminophen, Micronized Acetaminophen, ascorbic acid crystalline grade and ascorbic acid ultrafine grade were dry coated in the MAIC using the optimal operating conditions. Their flow and related properties were evaluated by flow from orifice through the Flodex device indicated as index (FI), angle of repose (AOR), conditioned bulk density (CBD), flow function coefficient (FFC) evaluated via shear testing, Carr index, as well as material properties such as the cohesion coefficient or the intrinsic shear strength using the Hosokawa powder tester, Quantachrome autotap, and the FT4 powder rheometer. Since flow and bulk density are two of the most important properties that determine the ease with which pharmaceutical powders can be stored, handled and processed, the results are presented as a phase map of inverse of cohesion which is a measure of flowability (Geldart et al., 2009) (or FFC) as a function of bulk density (Mullarney et al., 2011). Such phase maps are expected to provide quick, visual assessment of the extent of property enhancement due to dry coating.

2. Experimental

2.1. Materials

All of the raw materials used in this work are listed in Tables 1 and 2. Table 1 lists the average particle diameters, bulk

Table 1
The properties of the raw materials.

Material	Obtained from	Bulk density (g/ml)	Particle size (μm)				
			D_{10}	D_{50}	D_{43}	D_{32}	D_{90}
Ibuprofen 110 (IBU110)	Alfa Chem, U.S.A.	0.453	33.3	119.6	143.8	67.7	288.0
Ibuprofen 90 (IBU90)	BASF, U.S.A.	0.483	15.2	101.9	127.0	46.0	267.8
Ibuprofen 50 (IBU50)	BASF, U.S.A.	0.404	13.1	57.5	67.9	32.8	137.8
Coarse Acetaminophen (APAP)	AnMar International Ltd., U.S.A.	0.343	3.7	30.7	83.1	19.7	228.9
Micronized Acetaminophen (MAPAP)	Mallinckrodt Inc., U.S.A.	0.197	2.6	10.7	16.0	6.2	37.3
Ascorbic acid crystalline (AAC)	Ruger, U.S.A.	0.905	63.8	212.6	231.1	113.2	423.1
Ascorbic acid fine (AAF)	Ruger, U.S.A.	0.403	3.55	14.9	20.5	8.2	45.1
Cab-o-sil M-5P	Cabot Inc., U.S.A.	0.055	–	16.0 nm	–	–	–
Aerosil R972 Pharma	Evonik, U.S.A.	0.050	–	16.0 nm	–	–	–

Table 2
BET surface area, mechanical properties (hardness and elasticity) of the uncoated powders.

Material	BET surface area (m^2/g)	Hardness (GPa)	Elasticity (GPa)
Micronized Acetaminophen (MAPAP)	0.9014	1.0 ± 0.2[a]	1.7 ± 0.1[a]
Acetaminophen (APAP)	0.3269		
Ascorbic acid fine (AAF)	0.5467	5.0 ± 0.9[a]	4.6 ± 0.9[a]
Ascorbic acid crystalline (AAC)	0.0394		
Ibuprofen 50 (IBU50)	0.3096	0.6 ± 0.1[a]	1.9 ± 0.6[a]
Ibuprofen 90 (IBU90)	0.2208		
Ibuprofen 110 (IBU110)	0.1502		
Nano-silica	200	6.0	74

[a] These data obtained from literature in the work of Cao et al. (2010).

densities and the sources of the powders. Table 2 contains the surface area and mechanical properties of the materials. Most of these particles are brittle as indicated by the hardness and elasticity values in Table 2 when compared with aluminum particles with hardness of 11.8 GPa and elasticity of 70 GPa. These particles are non-spherical in shape as indicated by Fig. 1. The powders were dry coated with hydrophobic or hydrophilic silica using the MAIC.

2.2. Dry particle coating

The dry coating method is described in detail elsewhere (Ramlakhan et al., 2000; Yang et al., 2005; Beach et al., 2010), but it is briefly discussed here. Dry coating employed in this work utilizes the technique of magnetically assisted impaction coating (MAIC). It consists of a glass jar, containing the host and guest powders and magnetic particles made of barium ferrite coated with polyurethane, which is placed in a collar coil. Magnetic particles have irregular shapes and dimensions ranging from 0.8 to 1.4 mm. As voltage is applied, an oscillating magnetic field is generated by the coil, which accelerates and spins the magnets along with the host and guest particles in the jar. This promotes the collisions among the particles and with the walls of the vessel. During this process, guest particles get coated onto the surface of the host particles mainly due to impaction of fluidized magnetic particles. This

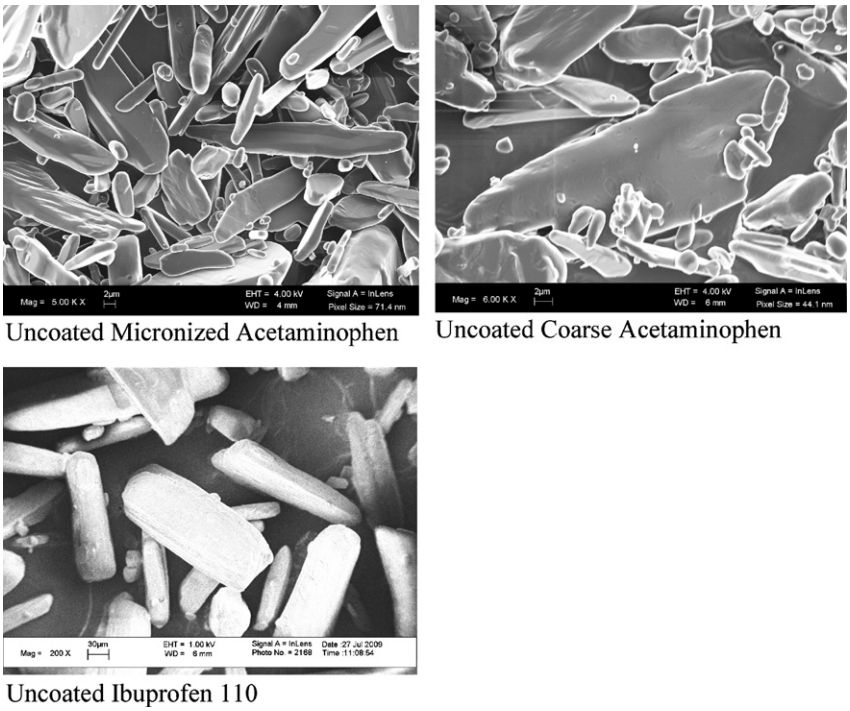

Fig. 1. Micrographs of uncoated particles showing the non-spherical shape, a slightly broad size distribution, and the superficially smooth surfaces.

device may be used with only small amount material, for example, 5 g, thus it is a material sparing technique. However, in our experiments, the batch size varied between 5 g and 10 g depending on the bulk density of the material.

2.3. Particle size analysis

Particle size and size distribution of the powders were measured in a Rodos/Helos unit (Sympatec, NJ, USA). The instrument has a powder dispersion component which works on the venture principle (RODOS) and a laser diffraction component (HELOS) with a parallel laser beam of 632.5 nm to measure particle sizes ranging from 0.1 μm to 3500 μm. The HELOS operating principle is based on the Fraunhofer Enhanced Evaluation (FREE) and Mie Extended Evaluation (MIEE) theories of light scattering. When in operation, the RODOS, through the expansion of compressed air accelerates the powder sample and causes dispersion by (1) particle–particle collisions, (2) particle–wall collisions, and (3) centrifugal forces due to strong velocity gradients. The dispersed aerosol is blown through the laser beam, analyzed by the HELOS and collected by suction using a vacuum.

In addition, pressure titration tests were performed by a series of repeated measurements at different dispersion pressures from 0.2 bar to 3.0 bar to study the powder dispersion and attrition due to dry coating.

2.4. Scanning electron microscopy (SEM)

The morphology of the particles was examined using a LEO 1530VP Field Emission Scanning Electron Microscope (FESEM) (LEO 1530 170, Carl Zeiss SMT Inc., MA, USA). Samples for FESEM were mounted on aluminum stubs with double-sided carbon tape and sputter-coated with carbon to enhance conductivity.

2.5. Flowability index (FI)

Hanson Flodex Powder Flowability Test Apparatus is used to measure the flowability index (FI). The FI is a measure of the flowability of the powder under gravity, for example, in die filling process. It is perhaps the simplest form of measure for minimum outlet diameter from a hopper. The Flodex set-up is a stainless steel cylinder with interchangeable stainless steel discs to be placed at the bottom, each with a different diameter hole at the center. The diameter of the holes ranges between 4 and 34 mm. The cylinder is mounted on a stand. A shutter controlled by a lever device is used to cover the hole while the powder is poured into the cylinder. The procedure used to measure the FI is as per the Flodex Operation Manual 21-101-000. To measure the FI, the powder is poured through a funnel into the center of the cylinder to 3/4 full and allowed to settle for 30 s. The shutter is opened quickly, without vibration to allow the powder to fall through. The FI is obtained when a powder freely falls 3 successive times through the hole in a specific disc.

2.6. Angle of repose (AOR)

Angle of repose (AOR) is the internal angle between the surface of a pile of powder and the horizontal axis. It is the easiest and most commonly used test for powder flowability. Measurement of AOR was performed according to the ASTM standard ASTM D6393-99 "Bulk Solids characterization by Carr Indices," using the Hosokawa powder tester (PT-N Powder characteristic Tester, Hosokawa Micron Powder System Co., Summit, NJ, USA). The measurement process involves the powder flowing through a funnel onto a circular plate to form a conical heap of powder for 180 s and suitable vibration rate depending on the powder. At the end of the run, the angle between the surface of the powder heap and the surface of the plate is measured with the measuring pin by aligning it parallel to the surface of the powder. For each powder, the procedure was repeated four times and an average value was reported as the AOR.

2.7. Bulk density for Carr index (CI)

Carr index is widely used to quantify the flow characteristics of particulate solid. It is calculated from bulk volume (V_i) and tapped volume (V_f), measured in this work with the Quantachrome Autotap using USP <616>Part II standard. In this process the powders were placed in a graduated cylinder and mounted on a tapping platform. The initial volume (V_i) of the sample was recorded, and the sample was tapped for 1250 times in increments of 500, 750 and 1250 taps. The final volume was also recorded (V_f) after 1250 taps. The Carr index (CI) was calculated from Eq. (1). It was introduced by Carr (1965) to characterize the flowability of bulk solids by using a scale of 0–100.

$$\mathrm{CI} = \frac{V_i - V_f}{V_f} \times 100 \quad (1)$$

All the MAIC processed APIs along with the unprocessed, as received APIs were characterized by the Carr index.

2.8. Powder characterization using FT4 powder rheometer

Shear test is an important and well accepted powder characterization method. It is based on the rheological and shear properties of a powder. The Freeman FT4 powder rheometer with shear cell module (Freeman Technology Ltd., Worcestershire, UK) was used for the following two tests for processed and unprocessed powders: (i) conditioned bulk density and (ii) shear cell test. Detailed experimental procedure is described elsewhere (Freeman, 2007).

For the measurements of conditioned bulk density, powders were gently filled in a 25 mm × 25 ml splitting cylindrical vessel. Conditioning was done using a specially design conditioning blade (helix angle of −5 degrees, 23.5 mm in diameter and the tip speed was 100 mm/s) which sliced the powder bed to remove any excess air and created a uniform powder bed in a low stress packing state. After the conditioning cycle, the cylindrical vessel was split to remove the excess mass of powder so that the volume of the remaining powder is 25 ml. The mass of the powder is automatically recorded by the computer and the bulk density is calculated. The test is repeated two more times and the average value is reported as the bulk density of the powder.

Based on the range of consolidation stresses normally encountered by pharmaceutical powders (low consolidation), for the shear test in the FT4 a 3 kPa pre-consolidation load was chosen. The powder was put into a 25 mm diameter glass vessel of 10 ml volume (25 mm × 10 ml split vessel) and conditioned using the conditioning blade. The powder bed was then pre-consolidated at a normal stress of 3 kPa using a vented piston, which is then replaced by a shear head with very small blades mounted on it. As the shear head touches the top of the powder bed, it applies the desired (as programmed) normal stress (σ) on the powder and induces the shear stress (τ). Several shear stresses (the point of incipient failure or the yield point) were found at different normal stresses (<pre-consolidation load). A Mohr's diagram was constructed using the FT4 software. The flow function coefficient FCC (defined as the ratio of consolidation stress to the unconfined yield stress), and cohesion coefficient (shear strength at zero normal stress) were obtained. A classification of powder flow behavior similar to that by Jenike has been defined by Schulze according to the FCCvalue:

Table 3
Variations of the operating parameters for optimizing the MAIC.

Parameters to study	Parameters variations
Magnet to powder ratio	0.5:1, 1:1, and 2:1
Processing time	5 min, 8 min, and 10 min
Coating type	Hydrophilic and Hydrophobic Silica
Powder type	Ibuprofen 110, Coarse, and Micronized Acetaminophen

Table 4
Statistical results of the effects of the four factors affecting the MAIC process.

Source	*P*-value	Effect
Magnet ratio (MR)	0.009	Significant
Processing time (PRT)	0.011	Significant
Coating type (CT)	0.046	Not that significant
Powder type (PT)	0.000	Significant

i.e., FCC < 1, not flowing; 1 < FCC < 2, very cohesive; 2 < FCC < 4, cohesive; 4 < FCC < 10, easy flowing and FCC > 10, free-flowing (Schulze, 2008).

2.9. Design of experiments (DoE) to study the parameters that affect surface modification in MAIC

In a previous optimization study (Ramlakhan et al., 2000), operating parameters for the MAIC system were optimized for non-pharmaceutical powders. In this study, design of experiments was used to optimize the factors that affect the MAIC process like guest particle type, processing time, and magnet to powder mass ratio (denoted as magnet ratio in next sections) of pharmaceutical powders. As indicated earlier, the model powders used are coarse Acetaminophen (APAP), Micronized Acetaminophen (MAPAP) and Ibuprofen 110 (IBU110). These three powders are representative of all of the other powders in Table 1. These powders are brittle as indicated by their elastic modulus and hardness in Table 2, with non-spherical shape as shown in Fig. 1.

Due to the brittle nature of these particles, and since particle attrition during processing is not desirable for the purpose of this surface modification, both the processing time and magnet ratio were not allowed to exceed the optimized values from earlier work (Ramlakhan et al., 2000) which were 10 min and a 2:1 ratio respectively. Hydrophobic silica (Aerosil R972) and hydrophilic silica (cab-o-sil MP5) were utilized in order to determine whether there is significant difference in flow improvement between them. Based on the different particle sizes and different surface chemistry of the model powders used, it is also expected that there will be a difference between them when processed. Using the Minitab 15, general full factorial design was performed and the experimental flow data obtained was analyzed at a significance level of $\alpha = 0.05$ to determine the significance of the parameters affecting the dry coating method. Table 3 shows the level of variations of the different processing parameters. Based on the statistical information obtained and flow data, optimized operating parameters for the dry coating process for such powders were obtained. The results are discussed in next section.

3. Results and discussions

3.1. Optimal amount of silica required for surface coating

To reduce the number of parameters in the DOE, an initial study (before any DOE experiments) was performed to standardize the amount of silica required for dry coating. This is one parameter that can easily be characterized using SEM and limited flow property tests, for example, AOR. In these and all subsequent experiments, the operating voltage of the MAIC electro-magnetic coil was set at 70 V so that over-heating of the coil was avoided yet we obtained sufficient excitation of the magnets. Fig. 2 is a plot of AOR of hydrophobic and hydrophilic silica coated ibuprofen (IBU110) as a function of weight percent of silica. The plot shows that there is no significant difference in flow improvement at the different coating levels. However, variability of measured AOR values is minimal in the case where 1 wt% nano-silica was used. Since the goal of this work is to standardize processing parameters, the one with the least variability was chosen. Thus, the amount of silica required to give the maximum flowability was set at 1 wt% for the DOE experiments. This is also consistent with recent work by Han et al. (2011). It is also noted that based on the previous studies (Yang et al., 2005); the flow improvement is a function of the surface area coverage (SAC) by silica and not directly with the amount of silica. To achieve the same SAC, amount of the silica or guest powder varies as a function of the surface area of the powder, which is related to average particle size. Earlier work also shows that for perfectly uniform and well-dispersed coating, the SAC should be between 20% and 100% to achieve maximum guest–guest contact when two coated particles come into contact (Chen et al., 2008). In practice, it is nearly impossible to achieve full dispersion. So one can utilize the amount of silica that corresponds to more than 100% coverage without making it excessive. Thus overall, there is reasonable latitude in the amount of SAC variation before it adversely impact the flow improvement. As will be seen in the next section, the 1 wt% silica was found to be adequate in flow improvement for the micronized APAP as well as coarse APAP, thus justifying the selection of a fixed 1 wt% of silica for this work.

3.2. Guest particle type

Using 1 wt% silica as a standard, the three model powders were dry coated using the MAIC. Statistical analysis of the AOR results indicated that there is no significant difference in flow improvement whether the coating was done with hydrophobic or hydrophilic silica (listed as coating type (CT)) as shown in Table 4, and is also confirmed by Fig. 2. All the other factors however, show a significant difference in flowability. Since there was no significant difference between the flow improvement of hydrophilic and hydrophobic coated powders, the rest of the plots in this work are only of hydrophilic silica coated powders. However, note that in general, coating with hydrophobic silica provides little better flow than with hydrophilic silica, which is preferred due to the reasons other than flow, for example, dissolution or wettability

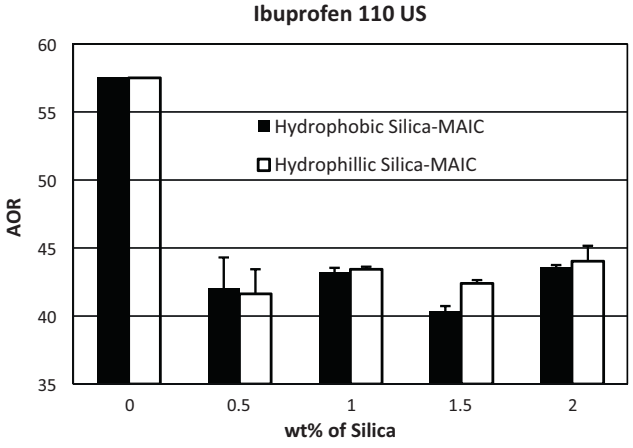

Fig. 2. The plot of AOR as a function of percent silica.

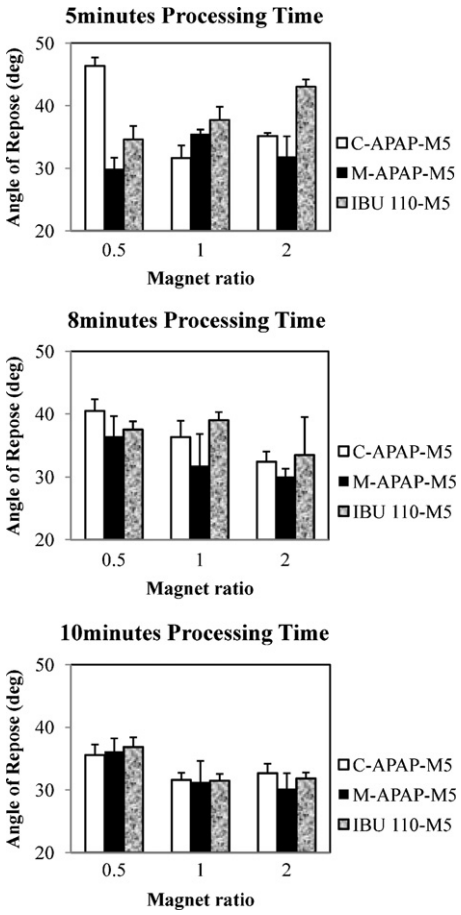

Fig. 3. Plots of AOR as a function of magnet ratio for 5, 8, and 10 min processing time.

improvement of the pharmaceutical powders. The effect of the rest of the parameters is discussed below.

3.3. Processing time

Based on the results from previous work (Ramlakhan et al., 2000), the processing times of 5, 8, and 10 min were investigated. The *P*-value in Table 4, for processing time is less than $\alpha = 0.05$. This implies that the duration of the coating process has a significant effect on the outcome. Fig. 3 shows a plot of AOR as a function of processing time. The plots of 5 and 8 min processing time show a significant scatter between the data of the different powders and inconsistent trends within the data of the same powder. However, all of the AOR results converged at 10 min of processing time, and follow a reasonable trend. Since the goal of this work is to set a standard operating time for all pharmaceutical powders, the value of 10 min was adopted as the processing time to evaluate the level of attrition generated at different magnet ratios as demonstrated in the next section.

3.4. Magnet to powder mass ratio

The amount of magnets used in MAIC significantly affects the level of attrition and surface area coverage of the host particle. This in turn affects the flow improvement characteristics of the powder. Magnet to powder ratios of 0.5:1, 1:1, and 2:1 were investigated and AOR plotted as a function of magnet ratio, MR (magnet to powder ratios) in Fig. 3. Since experiments with 5 min and 8 min results do not follow any particular trend, focus was placed only on the plot of 10 min processing time. For 10 min results, it can be observed that the variation between the data is minimal at all the magnet ratios. However, the SEM images in Fig. 4 show severe attrition of the host particles after dry coating with 2:1 magnet ratio, resulting in a change in both the particle size and shape. The rectangular shaped uncoated Ibuprofen 110 was attrited into irregular shaped and spherical particles. Riley and Mann (1972) showed that attrition of some elongated and plate like particles will lead to reduction in AOR. For proper scientific conclusions to be drawn between the uncoated and coated powders, only the effect of the surface modification should affect the results and not factors like attrition. Thus 2:1 magnet ratio is just not suitable for these powders.

Fig. 5 shows the plots of the mean particle size of uncoated and dry coated micronized APAP (a), coarse APAP (b), and Ibuprofen 110 (c) respectively as a function of dispersion pressure. It also shows pressure titration curves of MAPAP and APAP based on coarse 10% fraction particle size, d_{90}, in Fig. 5d and e. From Table 1, the average particle size (d_{50}) of coarse APAP is 30.7 μm, and micronized APAP is 10.7 μm. In pressure titration plots such as these, typically the values obtained at lower dispersion pressures indicate either the agglomerate sizes when the size decreases significantly with the pressure, or true particle sizes when the decrease is fairly small. On the other hand, as dispersion pressure increases, at some point the measured sizes decrease significantly, most likely indicating attrition. In all cases, however, the whole curve for dry coated powders is lower than the uncoated one, which represents attrition. Thus as can be seen in Fig. 5a and b, attrition of the particles generally increases with increasing the magnet loading. In both Fig. 5a and b, the particle sizes for 1:1 and 2:1 magnet ratio in MAIC show significant attrition of the original powder at about 70% and 60% of the original particle size respectively. However, particle size after dry coating with 0.5:1 magnet ratio shows about 13% attrition for both powders. Here we have taken the mean particle size after dry coating of these materials as those obtained at the lowest pressure

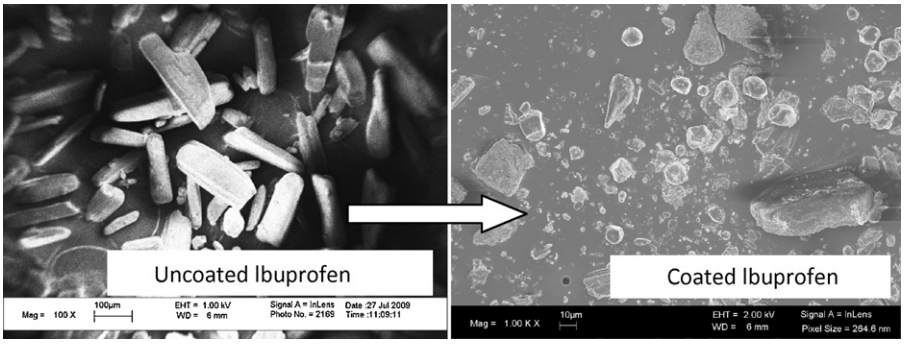

Fig. 4. SEM image of surface modified Ibuprofen 110, at 2:1 magnet ratio. The rectangular shaped uncoated Ibuprofen as shown in Fig. 1 has been attrited into a mixture of irregular shaped and spherical particles with an even wider size distribution.

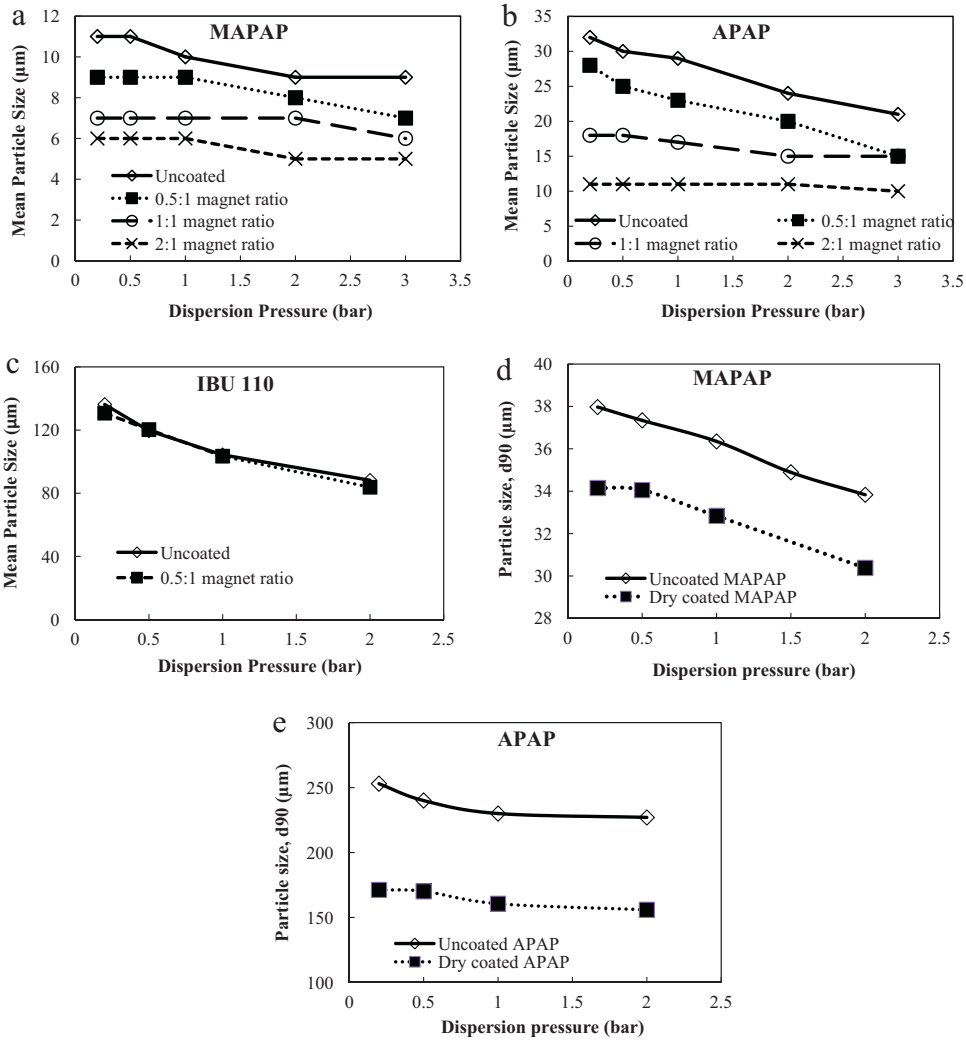

Fig. 5. (a–c) The mean particle size of uncoated and surface modified powder as a function of dispersion pressure for coarse APAP, micronized APAP, and Ibuprofen 110 and (d) shows the d_{90} plot of uncoated and coated MAPAP. (a–c) The effects of magnet size on attrition and (d, e) the effect of dry coating on dispersion of the powders.

(0.2 bar). On the other hand, Fig. 5c shows little attrition for Ibuprofen 110 when dry coated using magnet to powder ratio of 0.5:1. Based on the results obtained from the DOE study, the processing parameters of the MAIC for pharmaceutical powders has been set at 10 min processing time and 0.5:1 magnet to powder ratio. For MAPAP and APAP, d_{90} sizes are plotted in Fig. 5d and e, respectively, where dry coating was done at operating conditions of 10 min processing time and 0.5:1 magnet to powder ratio. These figures show severe agglomeration for uncoated powders, indicated through plot of d_{90} at low dispersion pressures, whereas, at higher dispersion pressures, attrition is observed. In contrast, the agglomerate sizes for both cases of dry coated powders are the same at dispersion pressures of 0.2 and 0.5 bar. Relatively flat curves at low pressures indicate excellent powder dispersion, and also indicate that there is less agglomeration (Han et al., 2011; Kaye et al., 2009), which we had also observed in SEM images (not shown here). One example of reduced agglomeration is seen from the SEM images of the fine grade of ascorbic acid (Fig. 7a). Thus these results indicate that dry coated powders have improved dispersibility requiring much lower dispersion pressure (hence lower energy) to achieve a fully dispersed dry state.

Fig. 6 shows the particle size distribution (PSD) of uncoated and dry coated APAP, IBU50, and AAC, respectively. These three powders are representative of the range of the mechanical characteristics (elasticity and hardness) of all of the APIs studied in this work. The plots show that for both uncoated and dry coated powders, APAP has a bimodal size distribution and IBU50 and AAC have unimodal size distribution. These figures also show the effect of the dry coating process on the particle size distribution. In the case of the AAC, there is basically no difference between the PSD of the uncoated and dry coated samples, which implies very little attrition during the dry coating process. APAP on the other hand shows a visible change of the mode in the left peak and a slight increase in the density distribution of the smaller particles after dry coating and IBU50 also show a slight decrease in the density distribution at the mode and a slight increase of smaller particles. This could be attributed to some small amount of attrition taking place during the dry coating process. As shown in Table 2, ascorbic acid has elasticity of about 5 GPa and hardness of about 4.6 GPa, and APAP has elasticity of about 1.7 GPa and hardness of about 1, and Ibuprofen has elasticity of about 1.9 GPa and hardness of about 0.6 GPa. Marsh 1964 defined a model which relates the yield pressure of a material to the modulus of elasticity and hardness. This model (Eq. (2)) was shown to have universal applicability by Tabor (1970):

$$\frac{H}{P_y} = 0.07 + 0.6 \ln \frac{E}{P_y} \quad (2)$$

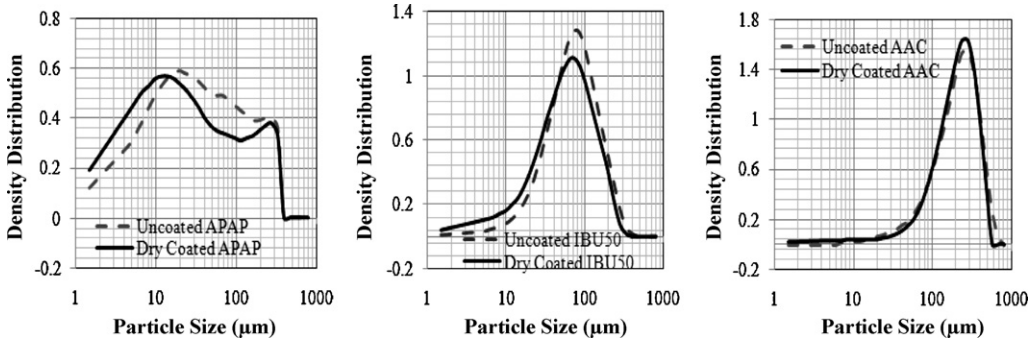

Fig. 6. Particle size distribution of uncoated and dry coated powders. All of the dry coating is done at the optimized operation parameters of the MAIC. The particle size distribution is obtained at 0.2 bar dispersion pressure.

where H is the hardness, E is the modulus of elasticity and P_y is the yield pressure, which is related to tendency to attrite. Thus the tendency of these particles to attrite could be attributed to their elasticity and hardness, which in this case means, powders with elasticity values of 2 GPa or less are more likely to attrite as compared to those with elasticities of about 5 GPa. In all cases however, the size distribution profile of all of the powders was unchanged after dry coating.

3.5. Packing and flow characterization

Using the optimized condition described above, several API powders were dry coated in MAIC (listed in Table 2 along with the corresponding BET surface area) using hydrophilic M5P nano-silica. Bulk scale measures like the conditioned bulk density, FFC, AOR, Carr index and FI; and material properties like the cohesion coefficient or intrinsic shear strength were obtained in addition to the, SEM images and particles sizes. Fig. 7 shows sample SEM images of two grades of uncoated and dry coated ascorbic acid powders. In both Fig. 7a and b, the left image is of the uncoated powders and the right image is the corresponding dry coated API powders. The images show the morphology, formed agglomerates of the uncoated particles and surface coating on dry coated particles. For Fig. 7a, the image of the uncoated AAF shows irregularly shaped and superficially smooth surface with mildly fused particles forming agglomerates (left figure), whereas, the dry coated image shows a dispersion of the individually coated particles with a mixture of distorted spherical, rectangular, square, and oval shapes (right figure). Fig. 7b shows the nearly cubic shape of both the coated and uncoated particles of the larger sizes AAC. The surface of the coated particles shows nano-sized asperities created by the nano-silica coating. As was shown in previous work (Chen et al., 2008, 2010; Jallo et al., 2010, 2011), the presence of these nano-particles on the surface of the host particles changes the contact geometry between the larger particles by reducing the contact area, resulting in a decrease in the adhesion force and improvement in flow properties.

The conditioned bulk densities (CBD) of the uncoated and dry coated powders measured with the FT4 are shown in Fig. 8. The plot is in increasing order of particle size of the powders in Table 2. In all cases except for AAC, there was an increase in bulk density for the dry coated powders. As shown in the SEM images in Fig. 7 and discussed in the experimental section, the dry coating method breaks up formed agglomerates of the uncoated powders as well as disperses the nano-silica on the surface of the individual particles. This results in better packing of the coated powder as compared to the uncoated because they form weak structures that easily collapse (Abdullah and Geldart, 1999). Thus, for a fixed volume, the mass of the dry coated powder is larger than the uncoated, resulting in higher bulk density.

Table 5
Theoretical surface area coverage of the API powders for 1 wt% silica based on D_{32} and BET surface area.

Material	SAC in % (based on D_{32})	SAC in % (based on BET surface area)
Micronized Acetaminophen (MAPAP)	46.2	86.0
Ascorbic acid fine (AAF)	78.0	110.2
Acetaminophen (APAP)	145.1	237.1
Ibuprofen 50 (IBU50)	209.3	288.6
Ibuprofen 90 (IBU90)	293.2	404.7
Ibuprofen 110 (IBU110)	431.2	595.0
Ascorbic acid crystalline (AAC)	1068.3	1529.0

For the case of AAC, there was a decrease in bulk density after dry coating. Table 2 shows the BET surface area for all the powders. AAC has the smallest BET surface area < 0.1 m^2/g and the SEM image in Fig. 9 shows the coated powder with agglomerates of excess nano-silica on the surface and in the bulk. This is an indication that the 1 wt% silica determined from the optimization process is excessive for such large particle size (212 μm). A simple analysis of the theoretical surface area coverage based on D_{32} as well as BET surface area is presented in Table 5. As can be seen, while the use of 1 wt% silica provides well over 100% surface area coverage for Ibuprofen powders, it is really excessive for coating of AAC. The result of the excess silica in the coated powder is reduced packing capability along with a decrease in mass for a fix volume as compared to the uncoated, hence the decrease in CBD of AAC. To rectify this, the theoretical amount required for 100% surface coverage of AAC based on its surface area using particle size (D_{32}) was calculated which is found to be 0.1 wt%. Dry coating of AAC with 0.1% of nano-silica increased the CBD from 0.905 g/ml (uncoated AAC) to 0.966 g/ml (dry coated with 0.1 wt% of silica). Subsequent bulk density data for AAC reported in this work is based on 0.1 wt% nano-silica coating. In contrast to the recent work on coating of lactose with Magnesium Stearate (Zhou et al., 2011), this study shows that increasing the amount of guest particles does not always guarantee an increase in bulk density.

The FFC of the uncoated and dry coated powders was obtained from the shear test results. The values are plotted in Fig. 10 in increasing order of particle size. For all the powders, the FFC of the dry coated is higher than corresponding uncoated API powder and it increases with increasing particle size for all powders. For the most cohesive powders, MAPAP, dry coating mildly improved the FFC and flow regime improved from very cohesive to cohesive region. But for AAF and APAP the flow regime improved from very cohesive to easy flowing powders and making these powders easier to handle in downstream processing. For the other APIs, particles with size greater than 30 μm, dry coating improved the flowability of the powders from easy flowing to free flowing. As discussed

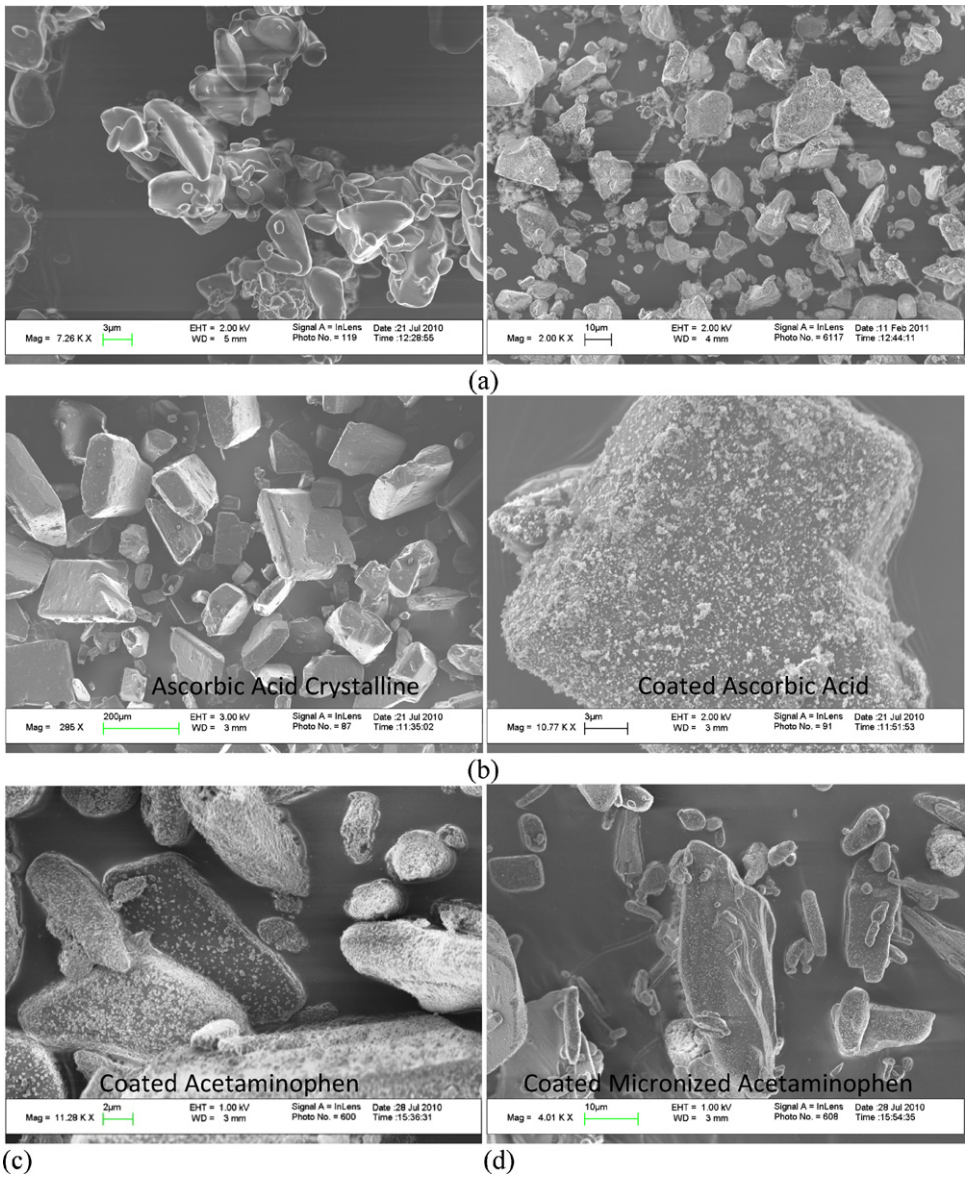

Fig. 7. Micrographs of uncoated and dry coated ascorbic acid (a) fine grade (AAF), (b) crystalline grade (AAC), (c) dry coated APAP, and (d) and MAPAP.

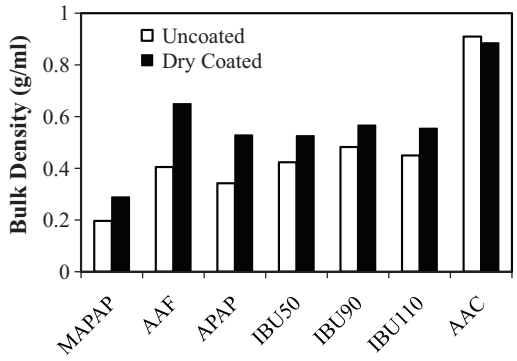

Fig. 8. Plot of bulk density of uncoated and dry coated powders.

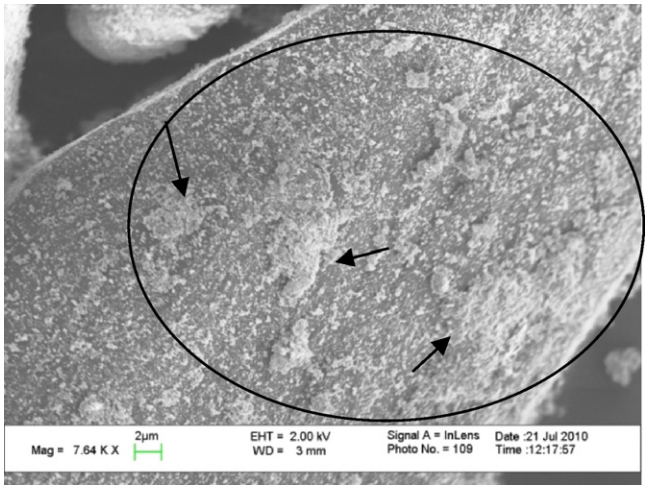

Fig. 9. Image of coated AAC, showing large agglomerates of nano-silica in excess of total surface coverage on the surface.

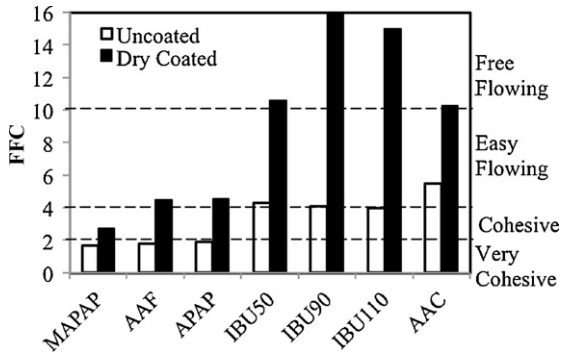

Fig. 10. Plot of flow function coefficient (FFC) for the uncoated and dry coated powders.

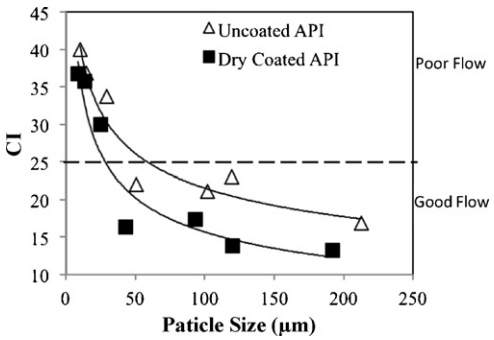

Fig. 12. A plot of Carr index as a function of particle size. The trend lines do not show clear distinction between coated and uncoated powders of <30 μm.

earlier, the improvement of the flow property (FFC) of the dry coated powders is due to the presence of the nearly spherical nano-silica on the surface of API particles (Chen et al., 2008; Yang et al., 2005). For the more cohesive powders, the dry coating process has not completely deagglomerated some of the aggregates of nano-silica, resulting in poorer coating quality that exposes some of API surface, which contributes to comparatively high adhesion force.

Looking at another metric, the AOR of the powders is plotted as a function of particle size in Fig. 11. The plot shows a general trend of decreasing AOR with increasing particles sizes. The AOR for all of the dry coated powders are lower than those of the uncoated, which is an indication of better flowability. The plot shows a clear distinction between the uncoated and dry coated powders.

The measured values for all the uncoated powders fall in the region of poor to exceedingly poor flow, and the dry coated values are in the fair to passable region. The AOR measurement involves making a conical pile the shape of which is affected by the strength of the adhesion force at the points of contact and the type of friction existing between the particles. Thus for the uncoated powders, the relatively large adhesion force between the particles results in them sticking together, creating steeper slopes and higher AOR values. In the case of the dry coated powders, smaller adhesion force leads to the formation of weaker structures that easily collapse as the particles settle on each other (Abdullah and Geldart, 1999) resulting in a smaller AOR.

A similar plot of CI as a function of particles size is shown in Fig. 12. In this plot however, all particles <30 μm are in the poor flow region whether they are dry coated or not, and particles >30 μm are in the good flow region whether dry coated or not. The trend lines also indicate that the distinction between the coated and uncoated powders is less apparent for finer sizes. The differences in the discernment provided by the AOR and CI values could be attributed to the methods used and associated error or sensitivity of each method. While the AOR is obtained from direct measurements using the Hosokawa powder tester, the CI is calculated from results from bulk and tapped volumes obtained from the Quantachrome Autotap employing USP standards. All of these methods have errors associated with their measured values. The error in estimating the AOR may arise from the subjective nature of the test, although the powder is conditioned as it passes through a sieve. The error for CI may be due to the way the powder is introduced into the test cylinder. Since there is no conditioning step involve in Autotap, the initial volume measured may be a little higher than the case with conditioning. Thus, the CI of very cohesive powders shows a little higher value than normal. This is the case with dry coated powders that are less than 30 μm.

Characterization of the powders based on their material properties, a plot of the "cohesion coefficient" or "intrinsic shear strength" as a function of the particles sizes is shown in Fig. 13. The cohesion coefficient is a result of the adhesion force between particles in a powder bed (Podczeck, 1998).

The plot shows a trend of decreasing cohesion with increasing particle size for all powders, and decreased cohesion in the case of the dry coated powders as compared to the uncoated. For sizes <30 μm, the uncoated particles are very cohesive. This is due to large van der Waals force between the particles which is in excess of the particle's weight. After dry coating, the cohesion force is mostly between the nano-silica coatings on the surface. This value is significantly smaller than that of the uncoated due to the reduction in contact area between the particles, hence the large reduction in cohesion in the dry coated powders.

For particles below 35 μm, uncoated powders are very cohesive, and in the size range between 50 μm and 150 μm, which are Ibuprofen of different size particles, they are still cohesive and are found to be at the boundary between quite cohesive and mildly cohesive. This observation is in line with what is observed in Fig. 10.

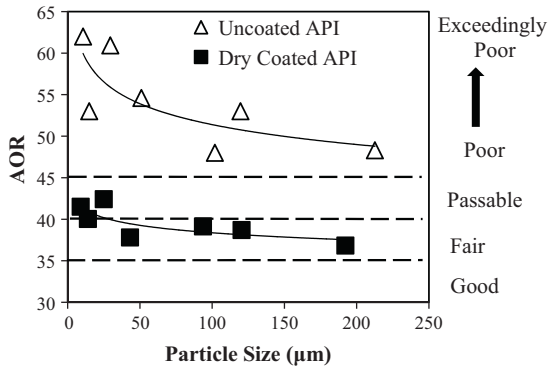

Fig. 11. The relationship between AOR and particle size. The trend lines show a clear distinction between the uncoated and dry coated powders.

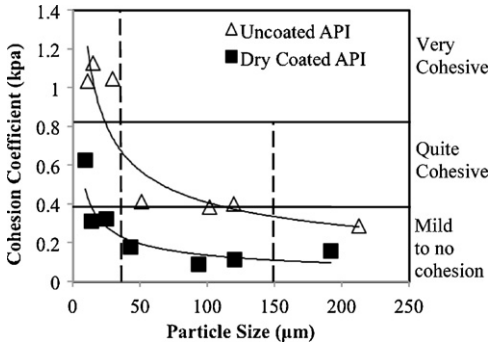

Fig. 13. A plot of cohesion coefficient as a function of particle size. The trend lines show a distinction between the uncoated and coated powders at all particle size.

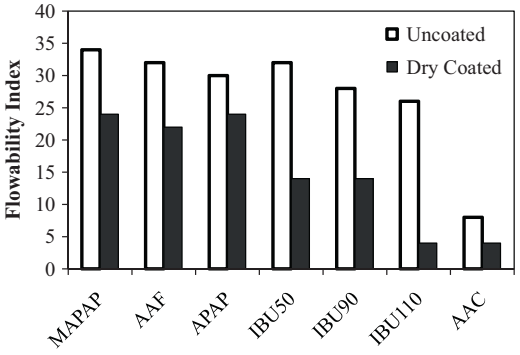

Fig. 14. A measure of the relative flowability of the powders as they flow through an orifice under gravity.

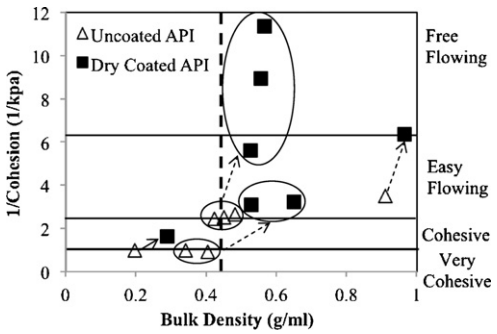

Fig. 15. A phase map of the inverse of cohesion coefficient as a function of conditioned bulk density of the uncoated and dry coated powders. Values of AAC are from 0.1 wt% silica and the rest are from 1 wt%.

On the other hand, with the exception of the finest API powder (MAPAP), all dry coated API powders are in the mild to no cohesion category, illustrating their tendency to flow freely under no consolidation. The dry coated powders >50 μm are all shown to be in the free flowing region in Fig. 10, and they are also having little cohesion as seen in Fig. 13.

Direct measure of flowability of the powders was made with the Flowdex and the results are represented in Fig. 14. The results show the FI of the uncoated and dry coated powders in increasing particle size. In this experiment, the best flowing powders easily pass through a 4 mm aperture and the worst ones flow through 34 mm aperture. All of the uncoated powders have FI greater than the corresponding dry coated ones. For the particles sizes of about 30 μm and below, the increase in flowability after dry coating is very good whereas that of the particles >50 μm is excellent, for example in the case of IBU110. The trend of flow improvements of the powders observed in this plot is similar to the ones observed in Figs. 12 and 13. The results presented here also corroborate the results from Beach et al. (2010), where they measured the flow rate of powder blends made from dry coated and common industrial practices of sieve blending and V-blending of Ibuprofen and APAP with silica using Near-Infrared Spectroscopy (NIR). They made blends with lactose having compositions of 5%, 25%, 50%, 75% and 100% of the drugs. It was shown that the blends of up to 75% dry coated ibuprofen at 0.5 wt% and 1.0 wt% silica flow through a funnel without any interruptions, at flow rates of 20.85 g/s and 31.5 g/s respectively. APAP blend containing 50% dry coated APAP at 0.5 wt% silica had a flow rate of 8.74 g/s and one containing 25% dry coated APAP at 1.0 wt% had a flow rate of 24.88 g/s. On the other hand, blends made at these same percentages without dry coating did not flow at all, indicating that dry coating also improves the flow rate.

3.6. *Property improvement after surface modification in a phase map*

As shown through various flow and density based properties, surface modification provides substantial overall improvements of API powders. These flow and packing properties can also be represented in terms of a more usable phase diagram in a manner similar to classic Geldart fluidization map (Geldart, 1973). Although there are several possible flow related indicators that can be selected to form a phase map, a simple 2-D phase diagram would be more convenient to pharmaceutical industry, where the dosage forms are predominantly solids (either tablets or powder-filled capsules). To help with the manufacturing decisions, such a phase map could be useful for examining not only the improvement in overall flow behavior due to dry coating but also its impact on the formulation strategy. Fig. 15 shows one possible phase map where inverse of cohesion is used as a flow indicator (Geldart et al., 2009) and conditioned bulk density is used as an indicator for packing tendency. The plot shows a dramatic increase in flow for AAF and APAP (paired in one ellipse) from the very cohesive region to the easy flowing region accompanied by an increased in bulk density. The MAPAP, shown by itself (lower left corner) also shows a significant improvement in both flow and bulk density. For the sake of being useful as a classification tool, the diagram is divided into several zones. A vertical line corresponds to CBD 0.45 g/ml beyond which direct compression is possible, the horizontal lines divide the total area into different degrees of cohesiveness. Though these lines are intended as preliminary guidelines, the main idea is to create different regimes for each processing route. For example, for tableting, the rectangle that is in the upper right side could represent the direct compression regime. All ibuprofen powders (shown together as triplet within one ellipse) as well as large sized ascorbic acid fall in to the direct compression regime after dry coating (as shown in Fig. 15). Moreover, dry coated AAF and APAP powders also fall in the free flowing region, indicating that they may work well for direct compression at comparatively high API content blends through selection of the appropriate type of excipient and composition. Likewise, the shift for MAPAP from lower-most left side to middle right side suggests that its blends may be amenable to roller compaction rather than needing routine wet granulation. Although the points shown in Fig. 15 are for 100% APIs, one could also show appropriate blends in such a diagram.

A second phase map is shown in Fig. 16 when FFC is plotted against CBD (Mullarney et al., 2011). The different horizontal zones are shown as suggested by Schwedes (1996). This diagram is also quite informative and is very similar to Fig. 15. It is clear that the lowest left-side rectangle most likely represents wet granulation regimes, while the upper, right-side rectangle clearly represents direct compression regimes.

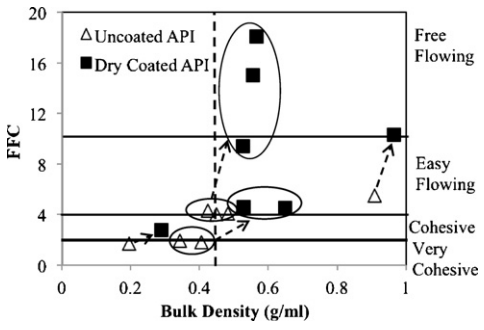

Fig. 16. A phase map of flow function coefficient (FFC) as a function of conditioned bulk density of the uncoated and dry coated powders. Values of AAC are from 0.1 wt% silica and the rest are from 1 wt%.

In both these examples, all APIs exhibit unidirectional property improvement; shown through the arrows running from bottom-left to top-right. Clearly, these phase-maps are shown as illustrative examples and only one of these two, depending on the user preference, would be sufficient for guidance regarding formulation or manufacturing decisions. One important observation that may be made for either of these diagrams is that three different types of drug particles show a general trend of increasing bulk density (or improving flow index) as particle size increases. However, the increase exhibited for uncoated drug powders is much weaker than those that are dry coated. In fact, dry coating makes these two properties more strongly dependent on particle size, and thus mostly diminishing the influence of individual API cohesion properties. That is very useful in designing formulations that reduce the influence of API's intrinsic flow and packing characteristics, and make them more dependent upon the particle size.

4. Conclusions

Magnetically assisted impaction coating (MAIC) was considered as a model dry coating device to carry out surface modification of three different types of pharmaceutical powders having different shapes, covering a range of particle sizes. MAIC was selected mainly because it has been previously shown to have a good potential for dry coating of API powders, and it is also a material sparing dry coating device. Although MAIC is a relatively gentler device, a limited design of experiment was conducted to establish a standardized MAIC processing procedure so as to limit the extent of powder attrition, while providing the most consistent improvement in angle of repose (AOR). Those experiments considered variables such as powder to magnet ratio, processing time, coating type and powder type. The fixed conditions utilized for the dry coating experiments include coil voltage setting at 70 V, operating time of 10 min and magnet to API powder ratio of 0.5:1.

Using the standard operating procedure for surface modification in MAIC, two sizes/grades of APAP, three sizes/grades of ibuprofen, and two sizes/grades of ascorbic acid powders were dry coated. The flow and packing properties of these dry coated APIs were characterized through various instruments to obtain the angle of repose, flowability index, the Carr index, conditioned bulk density, flow function coefficient, cohesion coefficient and particle sizes, and compared with those of the uncoated API. The general trend observed was an improvement of the dispersion, flow and packing properties after dry coating. These improvements are substantial and consistent across all powder characterization techniques used in this work. For flow, starting with the simple measurement of AOR to shear cell based measurements of FFC and cohesion coefficients that employ consolidation of the powders, all indicators showed a clear trend in flow improvement indicating that dry coating moved each powder from a poorer flow classification to an improved classification; i.e., FFC results show that a *very cohesive* powder (MAPAP) moves to the *cohesive* category, and *cohesive* powders moved to the *easy flowing* (AAF and APAP) or *free flowing* category (IBU and AAC). In addition to flow indicators, the material intrinsic property indicator such as cohesion coefficient, plotted as a function of particle size, gave a similar trend to those of bulk flow properties, such as AOR and CI. In terms of packing, bulk density measurements indicated substantial improvements, ranging from density increases of 10–80%. For many API powders, dry coating improves the conditioned bulk density of the powder to a value >0.45 g/ml, suggesting they pack very well and do not require roller compaction or other treatments to improve bulk density.

Since flow and packing are considered the two most important characteristics that determine the powder processibility, and, in the case of pharmaceutical manufacturing, the formulations and operations, the property improvement due to dry coating is illustrated in a phase map of inverse cohesion (or FFC) as a function of bulk density. Either of these phase maps provides an indication of the level of improvements due to dry coating; a significant positive shift may justify the need for use of dry coating. Dry coating also reduces the influence of individual API's intrinsic flow or packing property and makes them all a little stronger function of the particle size. It is suggested that in future work, regions are identified on these phase maps indicating suitability of operations such as direct compression, or need for granulation. Further, within granulation, depending on the flow and bulk density ranges, they could be classified as requiring wet or dry granulation. Thus it is hoped that such phase maps are useful in manufacturing decisions regarding (a) the need for dry coating, and (b) the extent to which dry coating allows for moving from wet granulation to roller compaction or to direct compression based formulations. Another possible and timely extension of this work would be to employ process analytical technology tools as suggested in Beach et al. (2010), where Near-IR was shown to be capable of monitoring flow rates and flow uniformity. Such work could facilitate quality by design by combining property enhancements at materials level with sensing that captures flow improvements.

Acknowledgements

This work has been funded in part by the National Science Foundation (NSF) through the ERC award, EEC-0540855. Additional funding from NSF awards, EEC-0552587, DMI-0506722, DGE-0504497, and EEC-0908889 is also acknowledged. Special thanks to Aveka, Inc., Woodbury, MN, for providing the use of the MAIC and Sympatec GmbH, for providing the use of the RODOS/HELOS system. Thanks are also due to Nancy Farlow for her editorial contributions, in particular about the graphical abstract.

References

Abdullah, E.C., Geldart, D., 1999. The use of bulk density measurements as flowability indicators. Powder Technol. 102, 151–165.
Beach, L., Ropero, J., Mujumdar, A., Alcalà, M., Romañach, R.J., Davé, R.N., 2010. Near-infrared spectroscopy for the in-line characterization of powder voiding. Part II. Quantification of enhanced flow properties of surface modified active pharmaceutical ingredients. J. Pharm. Innov. 5, 1–13.
Carr, R., 1965. Evaluating flow properties of solids. Chem. Eng. 72, 163–168.
Cao, X., Morganti, M., Hancock, B.C., Masterson, V.M., 2010. Correlating particle hardness with powder compaction performance. J. Pharm. Sci. 99, 4307–4316.
Chen, Y., Yang, J., Dave, R.N., Pfeffer, R., 2008. Fluidization of coated group C powders. AIChE J. 54, 104–121.
Chen, Y., Quintanilla, M.A.S., Dave, R., 2009. Pull-off force of dry coated fine powders under small consolidation. Phys. Rev. E 79, 041305-1–041305-14.
Chen, Y., Jallo, L., Quintanilla, M.A.S., Dave, R., 2010. Characterization of particle and bulk level cohesion reduction of surface modified fine aluminium powders. Colloids Surf. A: Phys. Eng. Aspects 361, 66–80.
Elbicki, J.M., Tardos, G.I., 1998. The influence of fines on the flowability of alumina powders in test hoppers. Powder Handl. Proc. 10, 147–149.
Fraige, F.Y., Langston, P.A., Matchett, A.J., Dodds, J., 2008. Vibration induced flow in hoppers: DEM 2D polygon model. Particuology 6, 455–466.
Freeman, R., 2007. Measuring the flow properties of consolidated, conditioned and aerated powders – a comparative study using a powder rheometer and a rotational shear cell. Powder Technol. 174, 25–33.
Geldart, D., 1973. Types of gas fluidization. Powder Technol. 7, 285–292.
Geldart, D., Abdullah, E.C., Verlinden, A., 2009. Characterization of dry powders. Powder Technol. 190, 70–74.
Ghoroi, C., Jallo, J.L., Gurumurthy, L., Patel, U., To, D., Beach, L., Dave, R.N., 2010a. Improvement in flowability and bulk density of pharmaceutical powders thorough surface modification. In: AIChE Annual Meeting, November 07–12, Salt Lake City, UT, USA.
Ghoroi, C., Bhakay, A., Dave, R.N., 2010b. Multifaceted characterization of flow, fluidization and packing properties of pharmaceutical powders for discerning the influence of surface modification. In: AIChE Annual Meeting, November 07–12, Salt Lake City, UT, USA.
Guerin, E., Tchoreloff, P., Leclerc, B., Tanguy, D., Deleuil, M., Couarraze, G., 1999. Rheological characterization of pharmaceutical powders using tap testing, shear cell and mercury porosimeter. Int. J. Pharm. 189, 91–103.

Han, X., Ghoroi, C., To, D., Chen, Y., Davé, R.N., 2011. Simultaneous micronization and surface modification for improvement of flow and dissolution of drug particles. Int. J. Pharm., Published online.
Jallo, L.J., Chen, Y., Bowen, J., Etzler, F., Dave, R.N., 2011. Prediction of inter-particle adhesion force from surface energy and surface roughness. J. Adhes. Sci. Technol. 18, 367–384.
Jallo, L.J., Schoenitz, M., Dreizin, E.L., Dave, R.N., Johnson, C.E., 2010. The effect of surface modification of aluminum powder on its flowability, combustion and reactivity. Powder Technol. 204, 63–70.
Kaya, B.H., Leblanc, J.E., Moxam, D., Zubac, D., 1983. The effect of vibration on the rheology of powders. Handl. Proc., 324–337.
Kaye, R.S., Purewal, T.S., Alpar, H.O., 2009. Simultaneously manufactured nano-in-micro (SIMANIM) particles for dry-powder modified-release delivery of antibodies. J. Pharm. Sci. 98, 4055–4068.
Kono, H.O., Huang, C.C., Xi, M., 1990. Function and mechanism of flow conditioners under various loading pressure conditions in bulk powders. Powder Technol. 63, 81–86.
Lecoq, O., Galet, L., Chamayou, A., 2011. High energy dry coating mixing: elements on velocities, temperatures and melting. Advanced Powder Technol. 22, 184–189.
Lindberg, N., Palsson, M., Pihl, A., Freeman, R., Freeman, T., Zetzener, H., Enstad, G., 2004. Flowability measurements of pharmaceutical powder mixtures with poor flow using five different techniques. Drug Dev. Ind. Pharm. 30, 785–791.
Molerus, O., 1978. Effect of interparticle cohesive forces on the flow behavior of powders. Powder Technol. 20, 161–175.
Mullarney, M.P., Beach, L.E., Davé, R.N., Langdon, B.A., Polizzi, M., Blackwood, D.O., 2011. Applying dry powder coatings to pharmaceutical powders using a comil for improving powder flow and bulk density. Powder Technol. 212, 397–402, doi:10.1016/j.powtec.2011.06.008.
Pfeffer, R., Dave, R.N., Wei, D., Ramlakhan, M., 2001. Synthesis of engineered particulates with tailored properties using dry particle coating. Powder Technol. 117, 40–67.
Pingali, K., Mendez, R., Lewis, D., Michniak-Kohn, B., Cuitino, A., Muzzio, F., 2011. Mixing order of glidant and lubricant – influence on powder and tablet properties. Int. J. Pharm. 409, 269–277.
Podczeck, F., 1998. Particle–particle Adhesion in Pharmaceutical powder Handling. Imperial College Press, London.
Ramlakhan, M., Wu, C.Y., Watano, S., Dave, R.N., Pfeffer, R.,1998. 90th Annual Meeting. AIChE.
Ramlakhan, M., Wu, Y., Watano, S., Dave, R.N., Pfeffer, R., 2000. Dry particle coating using magnetically assisted impaction coating: modification of surface properties and optimization of system and operating parameters. Powder Technol. 112, 137–148.
Riley, G.S., Mann, G.R., 1972. Effects of particle shape on angles of repose and bulk densities of a granular solid. Mater. Res. Bull. 7, 163–169.
Schulze, D., 2008. Powders and Bulk Solids – Behavior, Characterization, Storage and Flow. Springer, Berlin, Heidelberg, New York, Tokyo.
Schwedes, J., 1996. Measurement of flow properties of bulk solids. Powder Technol. 88, 285–290.
Tabor, D., 1970. The hardness of Solids. Rev. Phys. Technol. 1, 145–179.
Thalberg, K., Lindholm, D., Axelsson, A., 2004. Comparison of different flowability tests for powders for inhalation. Powder Technol. 146, 206–213.
Wassgren, C.R., Hunt, M.L., Freese, P.J., Palamara, J., Brennen, C.E., 2002. Effect of vertical vibration on hopper flows of granular materials. Phys. Fluids 14, 3439–3448.
Yang, J., Sliva, A., Banerjee, A., Dave, R., Pfeffer, R., 2005. Dry particle coating for improving the flowability of cohesive powders. Powder Technol. 158, 21–33.
Yu, A.B., Feng, C.L., Zou, R.P., Yang, R.Y., 2003. On the relationship between porosity and interparticle forces. Powder Technol. 130, 70–76.
Zhou, Q., Qu, L., Gengenbach, T., Denman, J.A., Larson, I., Stewart, P.J., Morton, D.A.V., 2011. Investigation of the extent of surface coating via mechanofusion with varying additive levels and the influences on bulk powder flow properties. Int. J. Pharm. 413, 36–43.